

Generative language modeling for antibody design

Richard W. Shuai^{a,1}, Jeffrey A. Ruffolo^{b,1}, and Jeffrey J. Gray^{b,c,2}

^aDepartment of Electrical Engineering and Computer Sciences, University of California, Berkeley, CA; ^bProgram in Molecular Biophysics, The Johns Hopkins University, Baltimore, MD; ^cDepartment of Chemical and Biomolecular Engineering, The Johns Hopkins University, Baltimore, MD

This manuscript was compiled on December 20, 2022

1 **Discovery and optimization of monoclonal antibodies for therapeutic applications relies on large sequence libraries, but is hindered by**
2 **developability issues such as low solubility, low thermal stability, high aggregation, and high immunogenicity. Generative language models,**
3 **trained on millions of protein sequences, are a powerful tool for on-demand generation of realistic, diverse sequences. We present**
4 **Immunoglobulin Language Model (IgLM), a deep generative language model for creating synthetic libraries by re-designing variable-length**
5 **spans of antibody sequences. IgLM formulates antibody design as an autoregressive sequence generation task based on text-infilling in**
6 **natural language. We trained IgLM on 558M antibody heavy- and light-chain variable sequences, conditioning on each sequence's chain type**
7 **and species-of-origin. We demonstrate that IgLM can generate full-length heavy and light chain sequences from a variety of species, as well as**
8 **infilled CDR loop libraries with improved developability profiles. IgLM is a powerful tool for antibody design and should be useful in a variety of**
9 **applications.**

antibodies | deep learning | language modeling

1 Introduction

2 Antibodies have become popular for therapeutics because of their diversity and ability to bind antigens with high
3 specificity (1). Traditionally, monoclonal antibodies (mAbs) have been obtained using hybridoma technology, which
4 requires the immunization of animals (2). In 1985, the development of phage display technology allowed for in vitro
5 selection of specific, high-affinity mAbs from large antibody libraries (3–5). Despite such advances, therapeutic mAbs
6 derived from display technologies face issues with developability, such as poor expression, low solubility, low thermal
7 stability, and high aggregation (6, 7). Display technologies rely on a high-quality and diverse antibody library as
8 a starting point to isolate high-affinity antibodies that are more developable (8). Synthetic antibody libraries are
9 prepared by introducing synthetic DNA into regions of the antibody sequences that define the complementarity-
10 determining regions (CDRs), allowing for human-made antigen-binding sites. However, the space of possible synthetic
11 antibody sequences is very large (diversifying 10 positions of a CDR yields $20^{10} \approx 10^{13}$ possible variants). To discover
12 antibodies with high affinity, massive synthetic libraries on the order of 10^{10} – 10^{11} variants must be constructed, often
13 containing substantial fractions of non-functional antibodies (2, 8).

14 Recent work has leveraged natural language processing methods for unsupervised pre-training on massive databases
15 of raw protein sequences for which structural data is unavailable (9–11). These works have explored a variety of
16 pre-training tasks and downstream model applications. For example, the ESM family of models (trained for masked
17 language modeling) have been applied to representation learning (9), variant effect prediction (12), and protein
18 structure prediction (13). Autoregressive language modeling, an alternative paradigm for pre-training, has also been
19 applied to protein sequence modeling. Such models have been shown to generate diverse protein sequences, which
20 often adopt natural folds despite diverging significantly in residue makeup (14, 15). In some cases, these generated
21 sequences even retain enzymatic activity comparable to natural proteins (16). Autoregressive language models have
22 also been shown to be powerful zero-shot predictors of protein fitness, with performance in some cases continuing to
23 improve with model scale (15, 17).

24 Another set of language models have been developed specifically for antibody-related tasks. The majority of prior
25 work in this area has focused on masked language modeling of sequences in the Observed Antibody Space (OAS)
26 database (18). Prihoda et al. developed Sapiens, a pair of distinct models (each with 569K parameters) for heavy
27 and light chain masked language modeling (19). The Sapiens models were trained on 20M and 19M heavy and light
28 chains respectively, and shown to be effective tools for antibody humanization. Ruffolo et al. developed AntiBERTy,
29 a single masked language model (26M parameters) trained on a corpus of 558M sequences, including both heavy and

The Johns Hopkins University has filed one or more patent application(s) related to this technology. R.W.S., J.A.R., and J.J.G. are named as inventors on these application(s).

¹R.W.S. and J.A.R. contributed equally to this work.

²To whom correspondence should be addressed. E-mail: jgray@jhu.edu

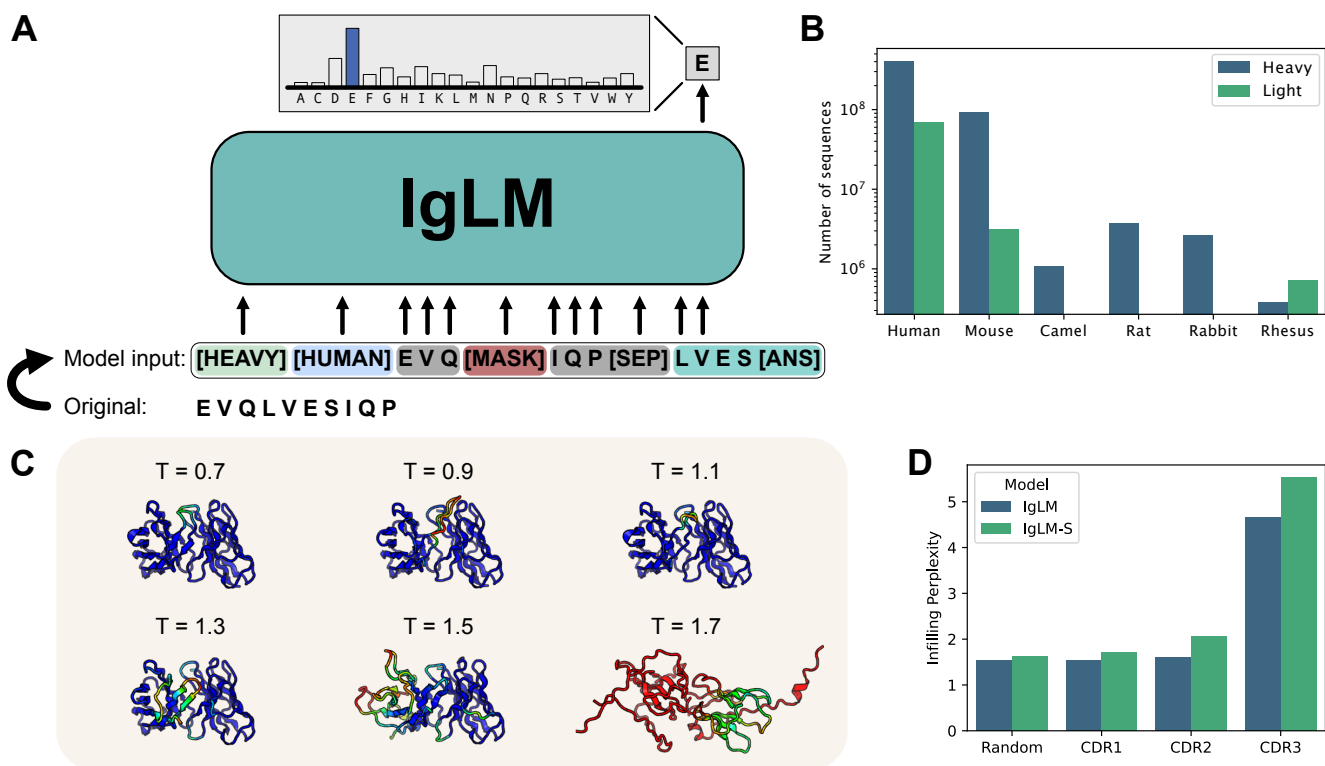


Fig. 1. Overview of IgLM model for antibody sequence generation. (A) IgLM is trained by autoregressive language modeling of reordered antibody sequence segments, conditioned on chain and species identifier tags. (B) Distribution of sequences in clustered OAS dataset for various species and chain types. (C) Infilling perplexity for IgLM and IgLM-S on holdout test dataset for CDR loops and random spans of 10-20 residues within sequences. (D) Effect of increased sampling temperature for full-length generation. Structures at each temperature are predicted by AlphaFold-Multimer and colored by prediction confidence (pLDDT), with blue being the most confident and red being the least.

light chains (20). AntiBERTy has been applied to representation learning for protein structure prediction (21). Leem et al. developed AntiBERTa, a single masked language model (86M parameters) trained on a corpus of 67M antibody sequences (both heavy and light). Representations for AntiBERTa were used for paratope prediction. Olsen et al. developed AbLang, a pair of masked language models trained on 14M heavy chains and 187K light chains, for sequence restoration (22). For sequence generation, autoregressive generative models have been trained on antibody sequences and used for library design (23, 24). Akbar et al. (23) trained an LSTM for autoregressive generation of CDR H3 loops and conducted an in silico investigation of their potential for binding antigens. Shin et al. (24) experimentally validated a set of nanobody sequences with generated CDR3 loops and showed promising improvements to viability and binding discovery when compared to traditional approaches, despite the library being over 1000-fold smaller. However, because this generative model was unidirectional, it could not be used to directly re-design the CDR3 loop *within the sequence*, and instead had to be oversampled to produce sequences matching the residues following the loop.

Here, we present Immunoglobulin Language Model (IgLM), a generative language model that leverages bidirectional context for designing antibody sequence spans of varying lengths while training on a large-scale natural antibody dataset. We show that IgLM can generate full-length antibody sequences conditioned on chain type and species-of-origin. Furthermore, IgLM can diversify loops on an antibody to generate high-quality libraries that display favorable biophysical properties while resembling human antibodies. IgLM should be a powerful tool for antibody discovery and optimization.

Results

Immunoglobulin language model. Our method for antibody sequence generation, IgLM, is trained on 558 million natural antibody sequences for both targeted infilling of residue spans, as well as full-length sequence generation. IgLM generates sequences conditioned on the species-of-interest and chain type (heavy or light), enabling controllable generation of antibody sequences.

Infilling language model. Design of antibody libraries typically focuses on diversification of the CDR loop sequences in order to facilitate binding to a diverse set of antigens. Existing approaches to protein sequence generation (including

54 antibodies) typically adopt left-to-right decoding strategies. While these models have proven effective for generation
55 of diverse and functional sequences, they are ill-equipped to re-design specific segments of interest within proteins.
56 To address this limitation, we developed IgLM, an infilling language model for immunoglobulin sequences. IgLM
57 utilizes a standard left-to-right decoder-only transformer architecture (GPT-2), but it is trained for infilling through
58 rearrangement of sequences. Specifically, we adopt the infilling language model formulation from natural language
59 processing (25), wherein arbitrary-length sequence segments (spans) are masked during training and appended to the
60 end of the sequence. By training on these rearranged sequences, models learn to predict the masked spans conditioned
61 on the surrounding sequence context.

62 To train IgLM, we collected antibody sequences from the Observed Antibody Space (OAS) (18). The OAS database
63 contains natural antibody sequences from six species: human, mouse, rat, rabbit, rhesus, and camel. To investigate
64 the impacts of model capacity, we trained two versions of the model: IgLM and IgLM-S, with 13M and 1.4M trainable
65 parameters, respectively. Both IgLM models were trained on a set of 558M non-redundant sequences, clustered at 95%
66 sequence identity. During training, we randomly masked spans of ten to twenty residues within the antibody sequence
67 to enable diversification of arbitrary spans during inference. Additionally, we conditioned sequences on the chain
68 type (heavy or light) and species-of-origin. Providing this context enables controllable generation of species-specific
69 antibody sequences. An example of training data construction is illustrated in Figure 1A. Unless otherwise specified,
70 we use the larger IgLM model for all experiments.

71 **IgLM generates foldable antibody sequences.** As an initial validation of the antibody sequence generation capabilities of
72 IgLM, we conducted a small scale investigation of full-length generation. Specifically, we investigated the impacts
73 of sampling temperature for tuning the diversity of generated sequences. Sampling temperature values above one
74 effectively flatten the amino acid distribution at each step of generation, resulting in more diverse sequences, while
75 temperature below one sharpens the distribution at each position, resembling a greedy decoding strategy. We
76 generated a set of full-length sequences at temperatures ranging from 0.7 to 1.7, providing the model with human
77 heavy and human light conditioning tags. Because IgLM was trained for sequence infilling, generated sequences
78 contain discontinuous segments of sequence segments, which we simply reordered to produce full-length antibodies.
79 Generated heavy and light chain sequences were paired according to sampling temperature and their structures were
80 predicted using AlphaFold-Multimer (26). In general, IgLM generates sequences with correspondingly confident
81 predicted structures at lower temperatures (up to 1.3), before beginning to degrade in quality at higher temperatures
82 (Figure 1C).

83 **Language modeling evaluation.** We evaluated IgLM as a language model by computing the per-token perplexity for
84 infilled spans within an antibody, which we term the *infilling perplexity*. Because the infilled segment is located at the
85 end of the sequences, computing the infilling perplexity is equivalent to taking the per-token perplexity after the
86 [SEP] token. We compared the infilling perplexity of IgLM and IgLM-S on a heldout test dataset of 30M sequences
87 (Figure 1D). Results are tabulated by CDR loop, as well as for spans selected randomly within the antibody sequence.
88 As expected, we observe greater perplexity for the CDR loops than the randomly chosen spans, which include the
89 highly conserved framework regions. The CDR3 loop, which is the longest and most diverse, has the highest infilling
90 perplexity. When we compare IgLM and IgLM-S, we observe that IgLM has a lower infilling perplexity for all CDR
91 loops, indicating that the larger IgLM model (with ten times more parameters) is better at modeling the diversity of
92 antibody sequences.

93 The diversity of antibody sequences varies by species and chain type. For example, heavy chains introduce
94 additional diversity into their CDR3 loops via D-genes, while some species (e.g., camels) tend to have longer loops. To
95 investigate how these differences impact the performance of IgLM in different settings, we also tabulated the heldout
96 set infilling perplexity by species and chain type. In general, both IgLM models achieve low infilling perplexity for
97 random spans across all species (Figure S1). For CDR1 and CDR2 loop infilling, perplexity values are typically lower
98 for human and mouse antibodies, which are disproportionately represented in the OAS database. In general, both
99 models still perform better on these loops than the more challenging CDR3 loops, regardless of species. One exception
100 is for rhesus CDR2 loops, on which IgLM-S performs considerably worse than the larger IgLM model. This appears to
101 be due to poor fitting of rhesus CDR L2 loops, as reflected in the similarity high infilling average perplexity observed
102 when tabulated by chain type (Figure S2). The highest infilling perplexity is observed for camel CDR3 loops, which
103 tend to be longer than other species. Across all species and chain types, the larger IgLM model achieves lower infilling
104 perplexity than IgLM-S, suggesting that further increasing model capacity would yield additional improvements.

105 **Controllable generation of antibody sequences.** Having demonstrated that IgLM can generate well-formed full-length
106 sequences, we next considered the controllability of IgLM for generating antibody sequences with specific traits.

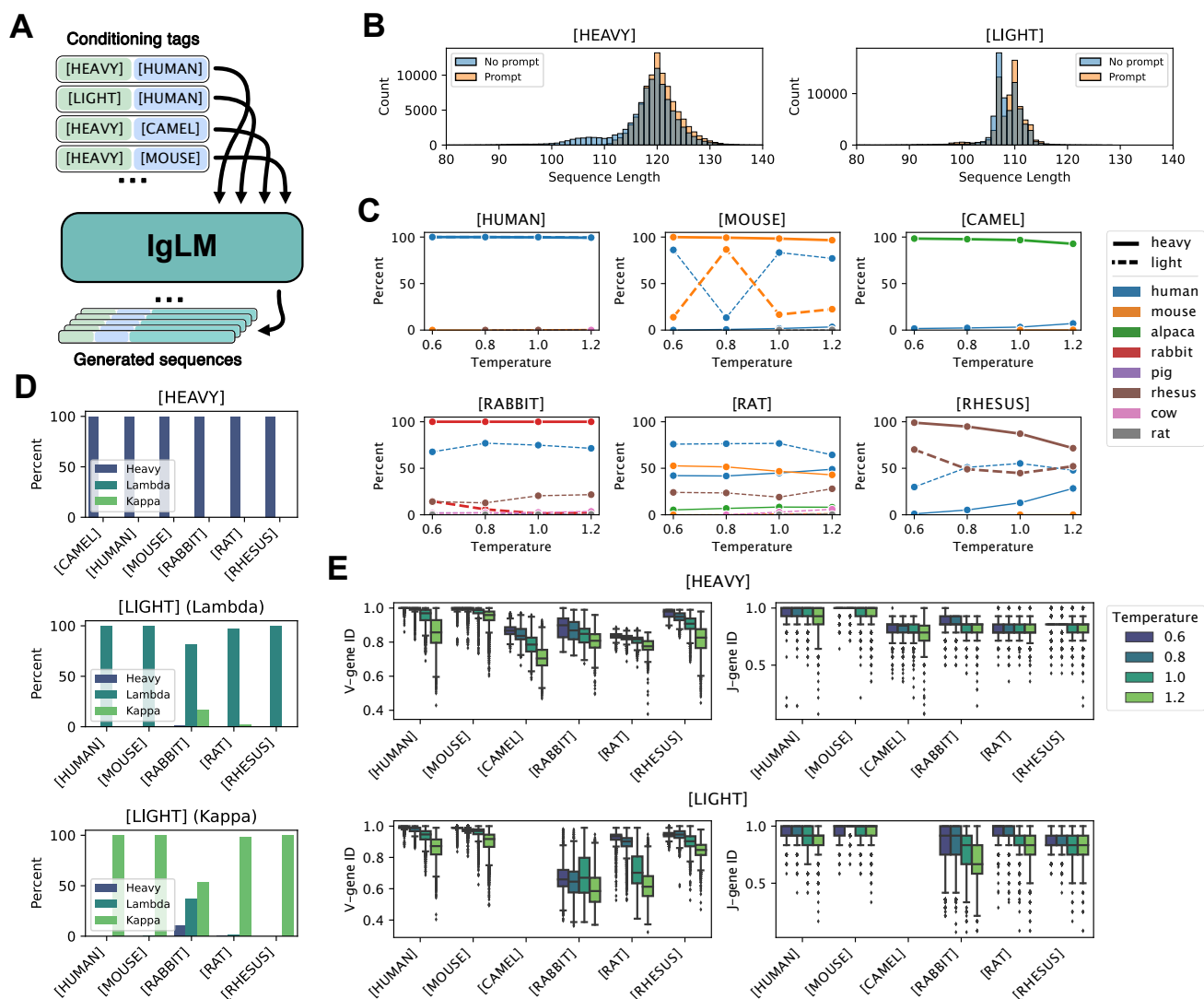


Fig. 2. Controllable antibody sequence generation. (A) Diagram of procedure for generating full-length antibody sequences given a desired species and chain type with IgLM. (B) Length of generated heavy and light with and without initial three residues provided (prompting). (C) Adherence of generated sequences to species conditioning tags. Each plot shows the species classifications of antibody sequences generated with a particular species conditioning tag (indicated above plots). Solid and dashed lines correspond to sequences generated with heavy- and light-chain conditioning, respectively. (D) Adherence of generated sequences to chain conditioning tags. Top plot shows the percentage of heavy-chain-conditioned sequences classified as heavy chains, for each species conditioning tag. Lower plots show the percentage of light-chain-conditioned sequences, further divided by whether initial residues were characteristic of lambda or kappa chains, classified as lambda or kappa chains. (E) Effect of sampling temperature on germline identity for generated heavy and light chain sequences. As sampling temperature increases, generated sequences diverge from the closest germline V- and J-gene sequences.

107 Controllable generation utilizes conditioning tags to provide the model with additional context about the expected
 108 sequence.

109 **Generating species- and chain-controlled sequences.** To evaluate the controllability of IgLM, we generated a set of 220K
 110 full-length sequences utilizing all viable combinations of conditioning tags, as well as a range of sampling temperatures
 111 (Figure 2A). For every species (except camel), we combined sampled with both heavy and light conditioning tags.
 112 For camel sequence generation, we only sampled heavy chains, as they do not produce light chains. To produce a
 113 diverse set of sequences for analysis, we sampled using a range of temperatures ($T \in \{0.6, 0.8, 1.0, 1.2\}$). Sampling
 114 under these conditions resulted in a diverse set of antibody sequences. However, we observed that the sequences
 115 frequently featured N-terminal truncations, a common occurrence in the OAS database used for training (22). For
 116 heavy chains, these N-terminal deletions appeared as a left-shoulder in the sequence length distribution (Figure 2B,
 117 left) with lengths ranging from 100 to 110 residues. For light chains, we observed a population of truncated chains
 118 with lengths between 98 and 102 residues (Figure 2B, right). To address truncation in generated sequences, we
 119 utilized a prompting strategy, wherein we initialize each sequence with a three-residue motif corresponding to the

120 species and chain type tags. Specific initialization sequences are documented in Table S2. For both heavy and light
121 chains, prompting with initial residues significantly reduced the population of truncated sequences (Figure 2B). For
122 the following analysis, we consider only sequences generated with prompting.

123 **Adherence to conditioning tags.** To evaluate the effectiveness of controllable generation, we considered the agreement
124 between the provided conditioning tags and the sequences produced by IgLM. For each generated sequence, we
125 classified the species (according to V-gene identity) and chain type using ANARCI (27). We note that the species
126 classes provided by ANARCI diverge in some cases from those provided by the OAS database, but there was a
127 suitable corresponding class for each conditioning token (e.g., alpaca for [CAMEL]). In Figure 2C, we show the makeup
128 of sequences for each species conditioning tag, according to sampling temperature. In each plot, the percentage of
129 heavy and light chain sequences classified as each species are indicated by solid and dashed lines, respectively. For
130 most species (human, mouse, camel, rabbit, rhesus), IgLM is able to successfully generate heavy chain sequences at
131 every temperature. The exception to this trend is rat sequences, for which we were unable to produce any sequences
132 that ANARCI classified as belonging to the intended species.

133 The ability to generate sequences is not directly explained by prevalence in the training dataset, as the model is
134 trained on an order of magnitude more rat heavy chain sequences than rhesus (Table S1). IgLM is generally less
135 effective at generating light chain sequences for most species. With the exception of human light chains, all species
136 have a large proportion of sequences classified as belonging to an unintended species (typically human). For mouse
137 and rhesus light chains, IgLM generates the correct species in 34.89% and 88.14% of cases, respectively (Table S3).
138 For rabbit and rat light chains, IgLM was not exposed to any examples during training. Interestingly, despite having
139 seen no such sequences during training, IgLM is capable of generating sequences classified by ANARCI as rabbit
140 light chains for 6.89% of samples (1,120 sequences). The majority of these sequences are cases where the model has
141 instead generated a rabbit heavy chain. However, for 35 of these 1,120 cases, IgLM has produced rabbit light chain
142 sequences. We further investigated the plausibility of these sequences by aligning to the nearest germline sequences
143 assigned by ANARCI with Clustal-Omega (28). The sequences appear to align well to rabbit germlines, though with
144 considerable mutations to the framework regions (Figure S3). To investigate the structural viability of the generated
145 rabbit light chain sequences, we predicted structures with IgFold (21). All structures were predicted confidently in
146 the framework residues, with the CDR loops being the most uncertain (Figure S4). Although rare (35 sequences out
147 of 20,000 attempts), these results suggest that IgLM is capable of generating rabbit light chain sequences despite
148 having never observed such sequences during training. This may be achieved by producing a consensus light chain,
149 with some rabbit-likeness conferred from the heavy chain examples.

150 We next evaluated the adherence of IgLM-generated sequences to chain type conditioning tags. In Figure 2D, we
151 show the percentage of sequences classified by ANARCI as heavy or light for each conditioning tag. Light chains are
152 further divided into lambda and kappa classes. When conditioned towards heavy chain generation, IgLM effectively
153 produces heavy chains for all species. For light chains, we observe a similar trend, with IgLM producing predominantly
154 light chain sequences for all species. Only for rabbit sequences do we observe a population of heavy chains when
155 conditioning for light chains. As noted above, these are cases where IgLM has instead produced a rabbit heavy chain.
156 When generating light chain sequences, we provide initial residues characteristic of both lambda and kappa chains in
157 equal proportion (Figure S2). For most species (except rabbit), the generated sequences are aligned with light chain
158 type indicated by the initial residues. However, as noted above, many of the light sequences for poorly represented
159 species are human-like, rather than resembling the desired species. Interestingly, these results suggest that the chain
160 type conditioning tag is a more effective prior for IgLM than species.

161 **Sampling temperature controls mutational load.** Increasing sampling temperature has the effect of flattening the probability
162 distribution at each position during sampling, resulting in a greater diversity of sequences. We evaluated the effect
163 of sampling temperature on the diversity of generated sequences by measuring the fractional identity to the closest
164 germline sequences using ANARCI (27). In Figure 2E, we show the germline identity for V- and J-genes for each
165 species and chain type. At the lowest sampling temperature ($T = 0.6$), IgLM frequently recapitulates germline
166 sequences in their entirety for some species (human, mouse, rhesus). As temperature increases, sequences for every
167 species begin to diverge from germline, effectively acquiring mutations. Interestingly, J-gene sequences typically
168 acquire fewer mutations than V-genes for both heavy and light chains. This is likely a reflection of the concentration
169 of CDR loops within the V-gene (CDR1 and CDR2). Only a portion of the CDR3 loop is contributed by the J-gene,
170 with the remaining sequence being conserved framework residues.

171 **Therapeutic antibody diversification.** Diversification of antibody CDR loops is a common strategy for antibody
172 discovery or optimization campaigns. Through infilling, IgLM is capable of replacing spans of amino acids within

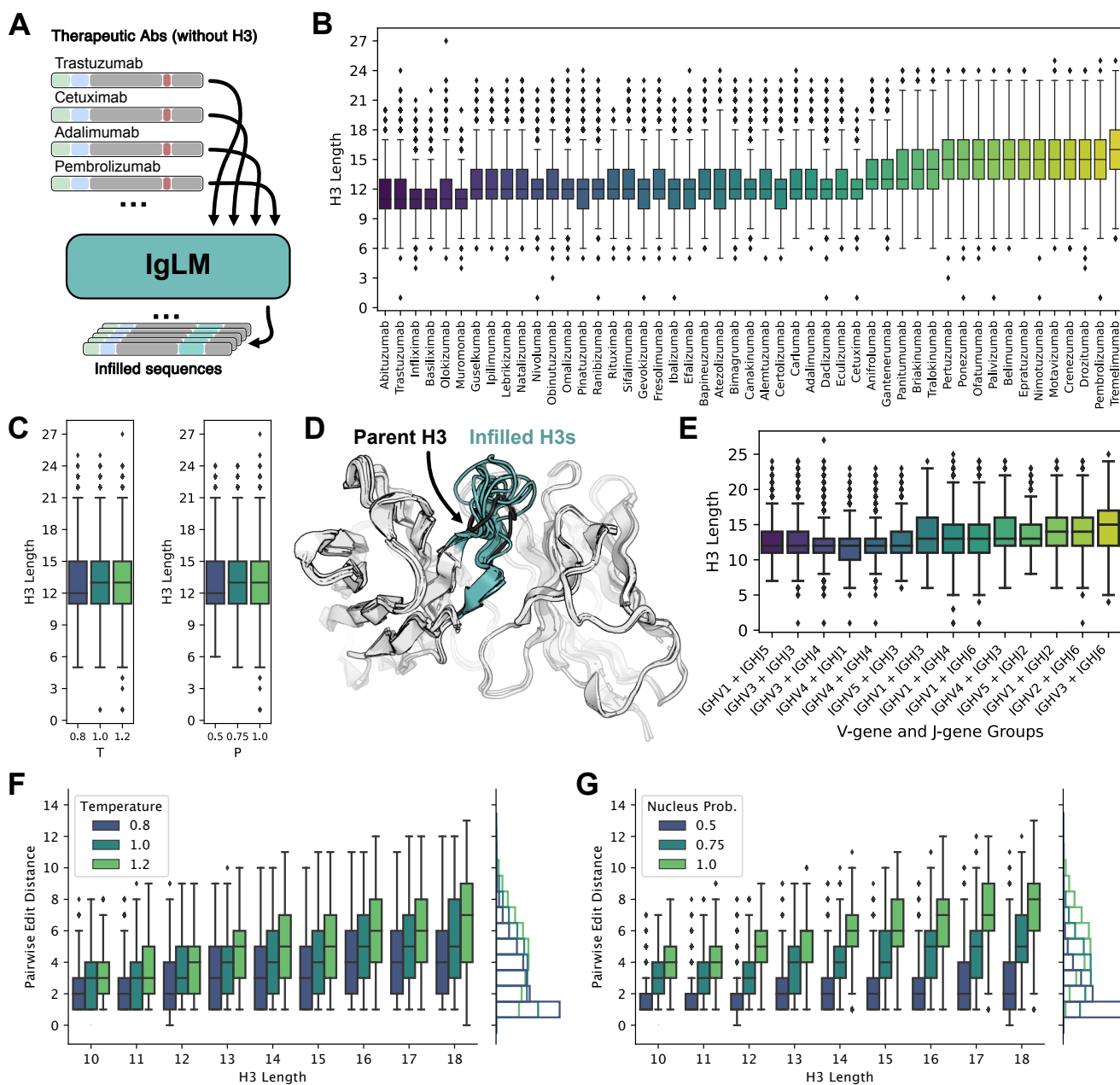


Fig. 3. Generation of infilled therapeutic antibody libraries. (A) Diagram of procedure for generating diverse antibody libraries by infilling the CDR H3 loops of therapeutic antibodies. (B) Distribution of infilled CDR H3 loop lengths for 49 therapeutic antibodies. (C) Relationship between sampling temperature (T) and nucleus probability (P) and length of infilled CDR H3 loops. (D) Infilled CDR H3 loops for trastuzumab therapeutic antibody adopt diverse lengths and conformations. Structures for infilled variants are predicted with IgFold. (E) Distribution of infilled CDR H3 loop lengths for therapeutic antibodies grouped by nearest germline gene groups. (F-G) Effect of sampling temperature (T) and nucleus probability (P) on diversity of infilled CDR H3 loops for lengths between 10 and 18 residues. Pairwise edit distance measures the minimum edits between each infilled loop to another in the same set of generated sequences (i.e., within the set of sequences produced with the same T and P parameters). For both parameters, less restrictive sampling produces greater infilled loop diversity.

173 antibody sequences, conditioned on the surrounding context. To demonstrate this functionality, we generated infilled
 174 libraries for a set of therapeutic antibodies and evaluated several therapeutically relevant properties.

175 **Infilled libraries for therapeutic antibodies.** To evaluate the utility of infilling with IgLM for diversifying antibody
 176 sequences, we created infilled libraries for 49 therapeutic antibodies from Thera-SAbDab (29). For each antibody, we
 177 removed the CDR H3 loop (according to Chothia definitions (30)) and generated a library of infilled sequences using
 178 IgLM (Figure 3A). To produce diverse sequences, we used a combination of sampling temperatures ($T \in \{0.8, 1.0, 1.2\}$)
 179 and nucleus sampling probabilities ($P \in \{0.5, 0.75, 1.0\}$). Nucleus sampling effectively clips the probability distribution
 180 at each position during sampling, such that only the most probable amino acids (summing to P) are considered. For

181 each of the 49 therapeutic antibodies, we generated one thousand infilled sequences for each combination of T and
182 P , totaling nine thousand variants per parent antibody. In Figure 3D, we show predicted structures (using IgFold
183 (21)) for a subset of ten infilled loops derived from the trastuzumab antibody. The infilled loops vary in length and
184 adopt distinct structural conformations. Across the infilled libraries, we see a variety of infilled CDR H3 loop lengths,
185 dependent on the parent antibody's surrounding sequence context (Figure 3B). The median length of infilled loops
186 across antibodies ranges from 11 to 16 residues. Interestingly, we observe little impact on the length of infilled loops
187 when varying the sampling temperature and nucleus probabilities (Figure 3C).

188 The distributions of infilled loop lengths vary considerably over the 49 therapeutic antibodies. Because IgLM
189 is trained on natural antibody sequences, we hypothesized that the model may be performing a sort of germline
190 matching, wherein sequences with similar V- and J-genes lead to similar distributions of loop lengths. To test this,
191 we identified the closest germline genes for each antibody with ANARCI (27). We then group parent antibodies
192 according to common V- and J-gene groups and compared the distributions of infilled loop lengths for each group
193 (Figure 3E). While there may be some tendency for similar V- and J-genes to lead to similar distributions of infilled
194 loop lengths, we observe considerable variation. This suggests that IgLM is not purely performing germline matching,
195 but rather is considering other properties of the parent antibody.

196 **Infilling generates diverse loop sequences.** Diverse loop libraries are essential for discovering or optimizing sequences
197 against an antigen target. To evaluate the diversity of infilled loops produced by IgLM, we measured the pairwise edit
198 distance between each loop sequence and its closest neighbor amongst the sequences generated with the same sampling
199 parameters. We then compared the diversity of sequences according to loop length and choice of sampling parameters
200 (Figure 3F-G). Generally, we observe that generated loops are more diverse at longer lengths, as expected given the
201 increased combinatorial complexity available as more residues are added. Increasing both sampling temperature and
202 nucleus probability results in a greater diversity of sequences. However, these parameters affect the relationship
203 between length and diversity in distinct ways. For a given loop length, increasing temperature produces more variance
204 in the pairwise edit distance, while increases to nucleus probability provides a more consistent increase in diversity
205 across loop lengths. Indeed, the marginal distribution of pairwise edit distance as nucleus probability is increased
206 produces a much larger shift (Figure 3G, marginal) than that of temperature (Figure 3F, marginal). In practice, a
207 combination of sampling parameters may be suitable for producing a balance of high-likelihood (low temperature and
208 low nucleus probability) and diverse sequences sequences.

209 **Infilled loops display improved developability.** Developability encompasses a set physiochemical properties – including
210 aggregation propensity and solubility – that are critical for the success of a therapeutic antibody. Libraries for
211 antibody discovery or optimization that are enriched for sequences with improved developability can alleviate the
212 need for time-consuming post-hoc engineering. To evaluate the developability of sequences produced by IgLM, we
213 used high-throughput computational tools to calculate the aggregation propensity (SAP score (31)) and solubility
214 (CamSol Intrinsic (32)) of the infilled therapeutic libraries. As a precursor to calculation of aggregation propensity, we
215 used IgFold (21) to predict the structures of the infilled antibodies (including the unchanged light chains). We then
216 compared the aggregation propensities and solubility values of the infilled sequences to those of the parent antibodies.
217 For aggregation propensity, we observed a significant improvement (negative is better) by infilled sequences over the
218 parent antibodies (Figure 4A, Figure S5). Similarly for solubility, infilled sequences tend to be more soluble than their
219 parent antibodies (Figure 4B, Figure S6). In both cases, the largest improvements tend to correspond to the shorter
220 loops. Further, we observe a positive correlation between improvements to aggregation propensity and solubility
221 (Figure 4C, Figure S7). These results suggest that infilling can be used to generate libraries enriched for sequences
222 with improved developability.

223 We next investigated whether choice of sampling parameters affects the developability of infilled sequences. When
224 we compared the aggregation propensity and solubility of infilled sequences according to the sampling temperature
225 and nucleus sampling probability, we found marginal practical differences (Figure S8). This is likely explained by
226 the relative consistency of infilled loop lengths across sampling parameters (Figure 3C). These results suggests that
227 developability should not be a concern when tuning the diversity of a generated library.

228 **Infilled loops are more human-like.** Therapeutic antibodies must be human-like to avoid provoking an immune response
229 and to be safe for use in humans. To evaluate the human-likeness of infilled sequences, we calculated the OASis
230 identity (at medium stringency) (19). OASis divides an antibody sequence into a set of 9-mers and calculates the
231 fraction that have been observed in human repertoires. Thus, higher OASis identity indicates a sequence that is more
232 similar to those produced by humans. When compared to their respective parent antibodies, sequences infilled by
233 IgLM were typically more human-like (Figure 4D). This is expected, given that IgLM is trained on natural human
234 antibodies. We also investigated the impact of sampling parameters on the human-likeness of infilled sequences.

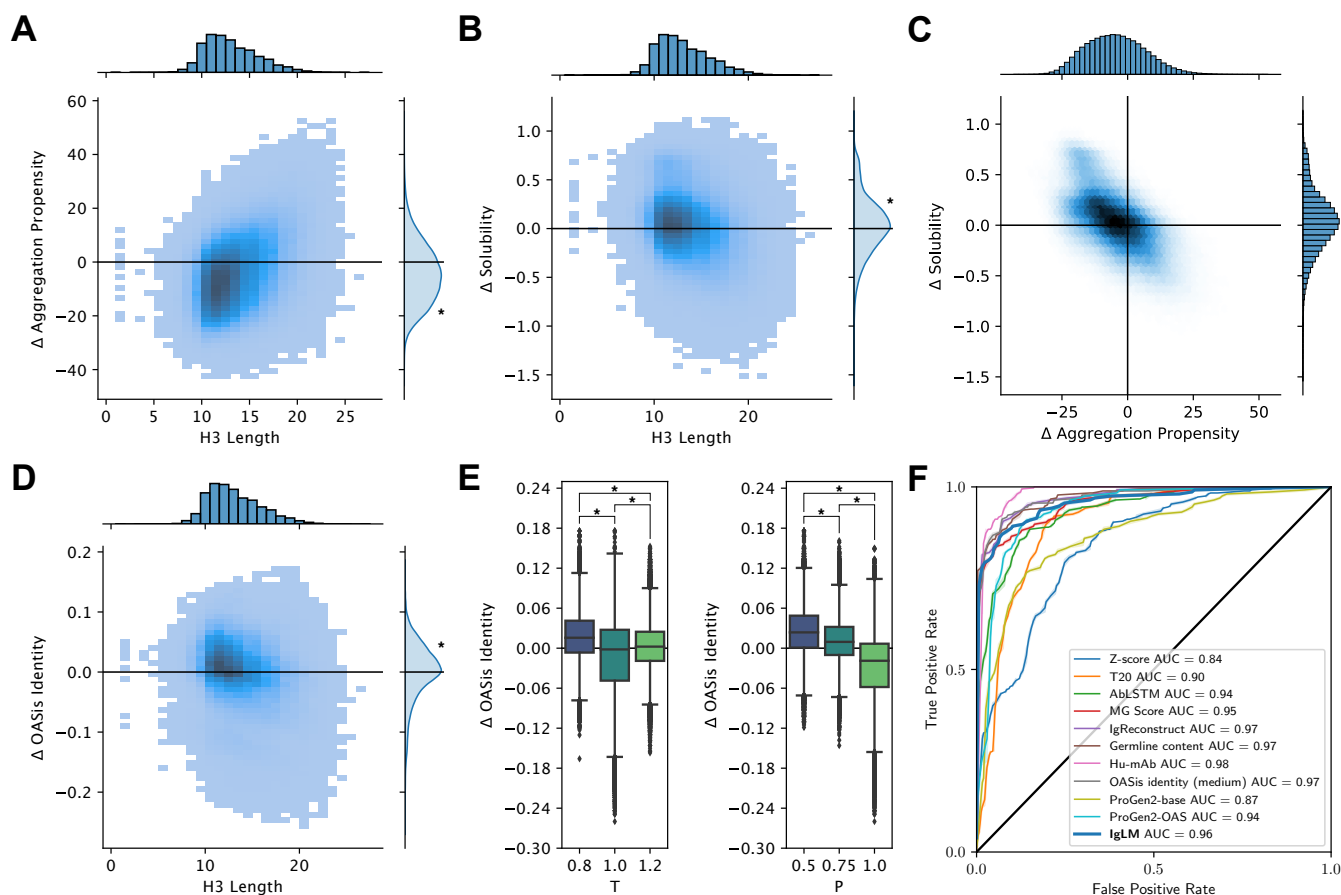


Fig. 4. Therapeutic properties of infilled antibody libraries. Asterisks indicate statistical significance ($p < 0.001$) from a one-sample t-test (A, B, D) or a two-sample t-test (E). (A) Change in predicted aggregation propensity of infilled sequences relative to their parent antibodies. Infilled sequences display reduced aggregation propensity (negative is improved), particularly for shorter loops. (B) Change in predicted solubility of infilled sequences relative to their parent antibodies. Infilled sequences display increased solubility (positive is improved). (C) Relationship between predicted changes in aggregation propensity and solubility for infilled sequence libraries. (D) Change in humanness of infilled sequences relative to their parent antibodies. Humanness is calculated as the OASis identity of the heavy chain sequence, with positive larger values being more humanlike. (E) Relationship between sampling temperature (T) and nucleus probability (P) and change in human-likeness (OASis identity) of infilled heavy chains relative to their parent sequences. (F) Receiver operating characteristic (ROC) curves for human sequence classification methods. The area under the curve (AUC) is shown for each method.

235 For both sampling temperature and nucleus probability, we find that less restrictive sampling tends to produce less
 236 human-like sequences (Figure 4E). For practical purposes, this suggests that sampling with lower temperature and
 237 nucleus probability may be more suitable when immunogenicity is a concern.

238 **Sequence likelihood is an effective predictor of humanness.** Likelihoods from autoregressive language models trained
 239 on proteins have been shown to be effective zero-shot predictors of protein fitness (15, 17). Antibody-specific language
 240 models in particular have been used to measure the "naturalness" of designed sequences (33), a measure related to
 241 humanness. To evaluate the effectiveness of IgLM for distinguishing human from non-human antibodies, we utilized
 242 the model's likelihood to classify sequences from the IMGT mAb DB (34). Sequences in this set span a variety of
 243 species (human and mouse) and engineering strategies (e.g., humanized, chimeric, felinized). We considered all
 244 sequences not specifically labeled as human to be non-human, and calculated a likelihood (conditioned on human
 245 species) for each. All sequences had both a heavy and light chain, for which we calculated separate likelihoods and
 246 then multiplied.

247 We compared the performance of IgLM to that of a number of other methods previously benchmarked by Prihoda et
 248 al. (19) using a receiver operating characteristic (ROC) curve (Figure 4F). The results here for alternative methods are
 249 adapted from those presented by Prihoda et al, but with several redundant entries removed to avoid double-counting.
 250 We additionally evaluated model likelihoods from ProGen2-base and ProGen2-OAS (15), which are models similar
 251 to IgLM that contain significantly more parameters (764M). ProGen2-base is trained on a diverse set of protein
 252 sequences, while ProGen2-OAS is trained on a dataset similar to IgLM (OAS clustered at 85% sequence identity). We
 253 find that IgLM is competitive with state-of-the-art methods designed for human sequence classification, though not

254 the best. Interestingly, IgLM outperforms ProGen2-OAS (ROC AUC of 0.96 for IgLM vs. 0.94 for ProGen2-OAS),
255 despite having significantly fewer parameters (13M vs. 764M). This may result from the different strategies for
256 constructing training datasets from OAS. By filtering at a less stringent 95% sequence identity, IgLM is likely exposed
257 to a greater proportion of human antibody sequences, which dominate the OAS database. These distinctions highlight
258 the importance of aligning training datasets with the intended application and suggest that training on only human
259 sequences may further improve performance for human sequence classification.

260 Discussion

261 Antibody libraries are a powerful tool for discovery and optimization of therapeutics. However, they are hindered by
262 large fractions of non-viable sequences, poor developability, and immunogenic risks. Generative language models
263 offer a promising alternative to overcome these challenges through on-demand generation of high-quality sequences.
264 However, previous work has focused entirely on contiguous sequence decoding (N-to-C or C-to-N) (15, 24). While
265 useful, such models are not well-suited for generating antibody libraries, which vary in well-defined regions within
266 the sequence, and for which changes may be undesirable in other positions. In this work, we presented IgLM, an
267 antibody-specific language model for generation of full-length sequences and infilling of targeted residue spans. IgLM
268 was trained for sequence infilling on 558M natural antibody sequences from six species. During training, we provide
269 the model with conditioning tags that indicate the antibody's chain type and species-of-origin, enabling controllable
270 generation of desired types of sequences.

271 Concurrent work on autoregressive language models for antibody sequence generation have been trained on similar
272 sets of natural antibody sequences and explored larger model sizes (15). However, models like ProGen2-OAS are
273 limited in utility for antibody generation and design, as they are difficult to guide towards generation of specific types
274 of sequences (e.g., species or chain types). Both this work and the ProGen2-OAS paper have utilized prompting
275 strategies to guide model generation towards full-length sequences. While these strategies may help in some cases
276 (particularly to overcome dataset limitations), significantly more reisdues may need to be provided to guide the
277 model towards a specific sequence type (e.g., human vs rhesus heavy chain). In contrast, by including conditioning
278 information for species and chain type in the model's training, IgLM is able to generate sequences of the desired type
279 without additional prompting. Still, as shown in this work, increasing the capacity of models like IgLM may lead to
280 better performance for sequence infilling (lower perplexity) and scoring (better likelihood estimation), a promising
281 direction for future work.

282 IgLM's primary innovation is the ability to generate infilled residue spans at specified positions within the antibody
283 sequence. In contrast to traditional generative language models that only consider preceding the residues, this enables
284 IgLM to generate within the full context of region to be infilled. We demonstate the utility of infilling by generating
285 libraries for 49 therapeutic antibodies. We found that IgLM was capable of generating diverse CDR H3 loop sequences,
286 and that diversity was largely tunable by choice of sampling parameters. Further, the infilled libraries possessed
287 desirable developability traits (aggregation propensity, solubility) while being more human-like on average than their
288 parent sequences. Notably, IgLM achieves these improvements over antibodies that are already highly optimized, as
289 all of the parent sequences have been engineered for mass-production and use in humans. Although we focused on
290 antibody loop infilling in this work, similar strategies may be useful for proteins generally. For example, a universal
291 protein sequence infilling model may be applicable to redesign of contiguous protein active sites or for generating
292 linkers between separate domains for protein engineering.

293 Code and Data Availability

294 Code and pre-trained models for IgLM are available at <https://github.com/Graylab/IgLM>. All generated sequences
295 and predicted structures will be deposited to Zenodo upon publication.

296 Methods

297 **Infilling formulation.** Designing spans of amino acids within an antibody sequence can be formulated as an infilling
298 task, similar to text-infilling in natural language. We denote an antibody sequence $A = (a_1, \dots, a_n)$, where a_i represents
299 the amino acid at position i of the antibody sequence. To design a span of length m starting at position j along the
300 sequence, we first replace the span of amino acids $S = (a_j, \dots, a_{j+m-1})$ with a single [MASK] token to form a sequence
301 $A_{\setminus S} = (a_1, \dots, a_{j-1}, [\text{MASK}], a_{j+m}, \dots, a_n)$. To generate reasonable variable-length spans to replace S given $A_{\setminus S}$, we seek
302 to learn a distribution $p(S|A_{\setminus S})$.

303 We draw inspiration from the Infilling by Language Modeling (ILM) framework proposed for natural language
304 infilling (25) to learn $p(S|A_{\setminus S})$. For assembling the model input, we first choose a span S and concatenate $A_{\setminus S}$,

[SEP], S , and [ANS]. We additionally prepend conditioning tags c_c and c_s to specific the chain type (heavy or light) and species-of-origin (e.g., human, mouse, etc.) of the antibody sequence. The fully formed sequence of tokens \mathbf{X} for IgLM is:

$$\mathbf{X} = (c_c, c_s, a_1, \dots, a_{j-1}, [\text{MASK}], a_{j+m}, \dots, a_n, [\text{SEP}], a_j, \dots, a_{j+m-1}, [\text{ANS}]) \quad [1]$$

We then train a generative model with parameters θ to maximize $p(\mathbf{X}|\theta)$, which can be decomposed into a product of conditional probabilities:

$$\max_{\theta} p(\mathbf{X}|\theta) = \max_{\theta} \prod_i p(\mathbf{X}_i | \mathbf{X}_{<i}, \theta) \quad [2]$$

Model implementation. The IgLM model uses a modified version of the GPT-2 Transformer decoder architecture (35) as implemented in the HuggingFace Transformers library (36). We trained two models, IgLM and IgLM-S, for sequence infilling. Hyperparameter details are provided in Table 1.

Table 1. IgLM model hyperparameters.

	IgLM	IgLM-S
Number of layers	4	3
Embedding dimension	512	192
Hidden dimension	512	192
Attention heads	8	6
Feed-forward dimension	2048	768
Total parameters	12,889,600	1,439,616

Antibody sequence dataset. To train IgLM, we collected unpaired antibody sequences from the Observed Antibody Space (OAS) (18). OAS is a curated set of over one billion unique antibody sequences compiled from over eighty immune repertoire sequencing studies. After removing sequences indicated to have potential sequencing errors, we were left with 809M unique antibody sequences. We then clustered these sequences using LinClust (37) at 95% sequence identity, leaving 588M non-redundant sequences. The distribution of sequences corresponding to each species and chain type are documented in Figure 1B and Table S1. The dataset is heavily skewed towards human antibodies, particularly heavy chains, which make up 70% of all sequences. We held out 5% of sequences as a test set to evaluate model performance. Of the remaining sequences, we used 558M sequences for training and 1M for validation.

Model training. During training, for each sequence $A = (a_1, \dots, a_n)$ we chose a mask length m uniformly at random from $[10, 20]$ and a starting position j uniformly at random from $[1, n - m + 1]$. We prepended two conditioning tags c_c and c_s denoting the chain type and species-of-origin of each sequence as annotated in the OAS database. Models were trained with a batch size of 512 and 2 gradient accumulation steps using DeepSpeed (38, 39). Training required approximately 3 days when distributed across 4 NVIDIA A100 GPUs.

ACKNOWLEDGMENTS. We thank Dr. Sai Pooja Mahajan and Dr. Rahel Frick for insightful discussions and advice. This work was supported by the National Science Foundation grant DBI-1950697 (R.W.S.) and National Institutes of Health grants R01-GM078221 (J.A.R.) and R35-GM141881 (J.A.R.). J.A.R. was supported as a Johns Hopkins-AstraZeneca Fellow. Computation was performed using the Advanced Research Computing at Hopkins (ARCH) core facility.

1. Masami Suzuki, Chie Kato, and Atsuhiko Kato. Therapeutic antibodies: their mechanisms of action and the pathological findings they induce in toxicity studies. *Journal of toxicologic pathology*, 28(3):133–139, 2015.
2. Sachdev S Sidhu and Frederic A Fellouse. Synthetic therapeutic antibodies. *Nature chemical biology*, 2(12):682–688, 2006.
3. John McCafferty, Andrew D Griffiths, Greg Winter, and David J Chiswell. Phage antibodies: filamentous phage displaying antibody variable domains. *nature*, 348(6301):552–554, 1990.
4. George P Smith. Filamentous fusion phage: novel expression vectors that display cloned antigens on the virion surface. *Science*, 228(4705):1315–1317, 1985.
5. Andrew D Griffiths, Samuel C Williams, Oliver Hartley, IM Tomlinson, P Waterhouse, William L Crosby, RE Kontermann, PT Jones, NM Low, and TJ at Allison. Isolation of high affinity human antibodies directly from large synthetic repertoires. *The EMBO journal*, 13(14):3245–3260, 1994.
6. Adriana-Michelle Wolf Pérez, Pietro Sormanni, Jonathan Sonne Andersen, Laila Ismail Sakhni, Ileana Rodriguez-Leon, Jais Rose Bjelke, Annette Juhl Gajhede, Leonardo De Maria, Daniel E Otzen, Michele Vendruscolo, et al. In vitro and in silico assessment of the developability of a designed monoclonal antibody library. In *MAbs*, volume 11, pages 388–400. Taylor & Francis, 2019.
7. Tushar Jain, Tingwan Sun, Stéphanie Durand, Amy Hall, Nga Rewa Houston, Juergen H Nett, Beth Sharkey, Beata Bobrowicz, Isabelle Caffry, Yao Yu, et al. Biophysical properties of the clinical-stage antibody landscape. *Proceedings of the National Academy of Sciences*, 114(5):944–949, 2017.
8. Juan C Almagro, Martha Pedraza-Escalona, Hugo Iván Arrieta, and Sonia Mayra Pérez-Tapia. Phage display libraries for antibody therapeutic discovery and development. *Antibodies*, 8(3):44, 2019.
9. Alexander Rives, Joshua Meier, Tom Sercu, Siddharth Goyal, Zeming Lin, Jason Liu, Demi Guo, Myle Ott, C Lawrence Zitnick, Jerry Ma, et al. Biological structure and function emerge from scaling unsupervised learning to 250 million protein sequences. *Proceedings of the National Academy of Sciences*, 118(15), 2021.
10. Ahmed Elnaggar, Michael Heinzinger, Christian Dallago, Ghalia Rihawi, Yu Wang, Llion Jones, Tom Gibbs, Tamas Feher, Christoph Angerer, Martin Steinegger, et al. Prottrans: towards cracking the language of life’s code through self-supervised deep learning and high performance computing. *arXiv preprint arXiv:2007.06225*, 2020.
11. Ali Madani, Bryan McCann, Nikhil Naik, Nitish Shirish Keskar, Namrata Anand, Raphael R Eguchi, Po-Ssu Huang, and Richard Socher. Progen: Language modeling for protein generation. *arXiv preprint arXiv:2004.03497*, 2020.

- 350 12. Joshua Meier, Roshan Rao, Robert Verkuil, Jason Liu, Tom Sercu, and Alexander Rives. Language models enable zero-shot prediction of the effects of mutations on protein function. *bioRxiv*, 2021.
- 351 13. Zeming Lin, Halli Akin, Roshan Rao, Brian Hie, Zhongkai Zhu, Wenting Lu, Allan dos Santos Costa, Maryam Fazel-Zarandi, Tom Sercu, Sal Candido, et al. Language models of protein sequences at
352 the scale of evolution enable accurate structure prediction. *bioRxiv*, 2022.
- 353 14. Noelia Ferruz, Steffen Schmidt, and Birte Höcker. Protgpt2 is a deep unsupervised language model for protein design. *Nature communications*, 13(1):1–10, 2022.
- 354 15. Erik Nijkamp, Jeffrey Ruffolo, Eli N Weinstein, Nikhil Naik, and Ali Madani. Progen2: exploring the boundaries of protein language models. *arXiv preprint arXiv:2206.13517*, 2022.
- 355 16. Ali Madani, Ben Krause, Eric R Greene, Subu Subramanian, Benjamin P Mohr, James M Holton, Jose Luis Olmos, Caiming Xiong, Zachary Z Sun, Richard Socher, et al. Deep neural language
356 modeling enables functional protein generation across families. *bioRxiv*, 2021.
- 357 17. Daniel Hesslow, Niccolò Zanichelli, Pascal Notin, Iacopo Poli, and Debora Marks. Rita: a study on scaling up generative protein sequence models. *arXiv preprint arXiv:2205.05789*, 2022.
- 358 18. Aleksandr Kovaltuk, Jinwoo Leem, Sebastian Kelm, James Snowden, Charlotte M Deane, and Konrad Krawczyk. Observed antibody space: a resource for data mining next-generation sequencing of
359 antibody repertoires. *The Journal of Immunology*, 201(8):2502–2509, 2018.
- 360 19. David Prihoda, Jad Maamary, Andrew Waight, Veronica Juan, Laurence Fayadat-Dilman, Daniel Svozil, and Danny Asher Bitton. Biophi: A platform for antibody design, humanization and humanness
361 evaluation based on natural antibody repertoires and deep learning. *bioRxiv*, 2021.
- 362 20. Jeffrey A Ruffolo, Jeffrey J Gray, and Jeremias Sulam. Deciphering antibody affinity maturation with language models and weakly supervised learning. *arXiv preprint arXiv:2112.07782*, 2021.
- 363 21. Jeffrey A Ruffolo and Jeffrey J Gray. Fast, accurate antibody structure prediction from deep learning on massive set of natural antibodies. *Biophysical Journal*, 121(3):155a–156a, 2022.
- 364 22. Tobias H Olsen, Iain H Moal, and Charlotte M Deane. Ablang: An antibody language model for completing antibody sequences. *bioRxiv*, 2022.
- 365 23. Rahmad Akbar, Philippe A Robert, Cédric R Weber, Michael Widrich, Robert Frank, Milena Pavlović, Lonneke Scheffer, Maria Chernigovskaya, Igor Snapkov, Andrei Slabodkin, et al. In silico proof of
366 principle of machine learning-based antibody design at unconstrained scale. In *Mabs*, volume 14, page 2031482. Taylor & Francis, 2022.
- 367 24. Jung-Eun Shin, Adam J Riesselman, Aaron W Kollasch, Conor McMahon, Elana Simon, Chris Sander, Aashish Manglik, Andrew C Kruse, and Debora S Marks. Protein design and variant prediction
368 using autoregressive generative models. *Nature communications*, 12(1):1–11, 2021.
- 369 25. Chris Donahue, Mina Lee, and Percy Liang. Enabling language models to fill in the blanks. *arXiv preprint arXiv:2005.05339*, 2020.
- 370 26. Richard Evans, Michael O'Neill, Alexander Pritzl, Natasha Antropova, Andrew W Senior, Timothy Green, Augustin Židek, Russell Bates, Sam Blackwell, Jason Yim, et al. Protein complex prediction
371 with alphafold-multimer. *BioRxiv*, 2021.
- 372 27. James Dunbar and Charlotte M Deane. Anarci: antigen receptor numbering and receptor classification. *Bioinformatics*, 32(2):298–300, 2016.
- 373 28. Fabian Sievers and Desmond G Higgins. Clustal omega, accurate alignment of very large numbers of sequences. In *Multiple sequence alignment methods*, pages 105–116. Springer, 2014.
- 374 29. Matthew IJ Raybould, Claire Marks, Alan P Lewis, Jiye Shi, Alexander Bujotzek, Bruck Taddese, and Charlotte M Deane. Thera-sabdbab: the therapeutic structural antibody database. *Nucleic acids
375 research*, 48(D1):D383–D388, 2020.
- 376 30. Cyrus Chothia and Arthur M Lesk. Canonical structures for the hypervariable regions of immunoglobulins. *Journal of molecular biology*, 196(4):901–917, 1987.
- 377 31. Naresh Chennamsetty, Vladimir Voynov, Veysel Kayser, Bernhard Helk, and Bernhard L Trout. Prediction of aggregation prone regions of therapeutic proteins. *The Journal of Physical Chemistry B*,
378 114(19):6614–6624, 2010.
- 379 32. Pietro Sormanni, Francesco A Aprile, and Michele Vendruscolo. The camsol method of rational design of protein mutants with enhanced solubility. *Journal of molecular biology*, 427(2):478–490, 2015.
- 380 33. Sharrol Bachas, Goran Rakocevic, David Spencer, Anand V Sastry, Robel Haile, John M Sutton, George Kasun, Andrew Stachyra, Jahir M Gutierrez, Edriss Yassine, et al. Antibody optimization
381 enabled by artificial intelligence predictions of binding affinity and naturalness. *bioRxiv*, 2022.
- 382 34. C Poirou, Y Wu, C Ginestoux, F Ehrenmann, P Duroux, and MP Lefranc. Imgt/mab-db: the imgt® database for therapeutic monoclonal antibodies. *Poster no101*, 11, 2010.
- 383 35. Alec Radford, Jeffrey Wu, Rewon Child, David Luan, Dario Amodei, Ilya Sutskever, et al. Language models are unsupervised multitask learners. *OpenAI blog*, 1(8):9, 2019.
- 384 36. Thomas Wolf, Julien Chaumond, Lysandre Debut, Victor Sanh, Clement Delangue, Anthony Moi, Pierric Cistac, Morgan Funtowicz, Joe Davison, Sam Shleifer, et al. Transformers: State-of-the-art
385 natural language processing. In *Proceedings of the 2020 Conference on Empirical Methods in Natural Language Processing: System Demonstrations*, pages 38–45, 2020.
- 386 37. Martin Steinegger and Johannes Söding. Clustering huge protein sequence sets in linear time. *Nature communications*, 9(1):1–8, 2018.
- 387 38. Samyam Rajbhandari, Jeff Rasley, Olatunji Ruwase, and Yuxiong He. Zero: Memory optimizations toward training trillion parameter models. In *SC20: International Conference for High Performance
388 Computing, Networking, Storage and Analysis*, pages 1–16. IEEE, 2020.
- 389 39. Jie Ren, Samyam Rajbhandari, Reza Yazdani Aminabadi, Olatunji Ruwase, Shuangyan Yang, Minjia Zhang, Dong Li, and Yuxiong He. Zero-offload: Democratizing billion-scale model training. *arXiv
390 preprint arXiv:2101.06840*, 2021.